IEEE Access
Multidisciplinary | Rapid Review | Open Access Journal

IEEE POWER & ENERGY SOCIETY SECTION

Received 24 July 2022, accepted 17 August 2022, date of publication 19 August 2022, date of current version 26 August 2022.

Digital Object Identifier 10.1109/ACCESS.2022.3200370

APPLIED RESEARCH

Coordinated Low Voltage Ride-Through of MMC-HVDC Transmission System and Wind Farm With Distributed Braking Resistors

XIAOHE WANG[1,2,3], RENXIN YANG[2], (Member, IEEE), ZHAOHUI SHI[1,3], XU CAI[2], (Senior Member, IEEE), XIANQIANG SHI[2], (Graduate Student Member, IEEE), AND YUWEI CHEN[1,3]

[1]Key Laboratory of Far-Shore Wind Power Technology of Zhejiang Province, Hangzhou 311122, China
[2]Key Laboratory of Control of Power Transmission and Conversion, Shanghai Jiao Tong University, Shanghai 200240, China
[3]Powerchina Huadong Engineering Corporation Ltd., Hangzhou 311122, China

Corresponding author: Renxin Yang (frank_yang@sjtu.edu.cn)

This work was supported by the National Key Research and Development Plan of China under Grant 2021YFB2400600.

ABSTRACT Modular multilevel converter-based high-voltage direct current (MMC-HVDC) transmission is becoming a trend in offshore wind-farm integration. However, the large DC-side energy dissipation equipment, which is utilized to dissipate surplus wind power under grid fault conditions, will largely increase the cost of MMC-HVDC systems. To reduce the cost, a novel low voltage ride-through (LVRT) strategy is proposed in this paper. When a grid fault occurs and the DC voltage exceeds the limit, the sending end converter is controlled to reduce the AC voltage of the wind farm. The LVRT of the wind generators will be activated, and the output active power of the wind farm is reduced. With this coordination, the DC-side energy dissipation equipment only needs to dissipate surplus power in the early stage of the grid fault before the output active power of the wind farm drops. Therefore, the heat generated by braking resistors can be significantly reduced. On this basis, the braking resistors can be distributed into the submodules of the receiving end converter (REC) station. The LVRT problem can be solved without building an individual energy dissipation station. Using the proposed coordination strategy, the construction cost of the MMC-HVDC system with offshore wind farm integration can be significantly reduced.

INDEX TERMS HVDC transmission, low voltage ride-through, modular multilevel converters, offshore wind farm.

I. INTRODUCTION

Offshore wind power is regarded as an effective solution to the energy crisis[1]. For distant offshore wind farms (OWFs), the modular multilevel converter-based high-voltage direct current (MMC-HVDC) transmission is becoming a competitive choice compared to its high-voltage AC (HVAC) transmission counterpart [2], [3], which has capacitive charging effects of HVAC submarine cables.

In recent years, the scale, voltage level, and capacity of MMC-HVDC projects with OWF integration have rapidly increased [4], [5]. However, owing to the low voltage and current withstand capability of power electronic devices, the low voltage ride-through (LVRT) of the MMC-HVDC system and the OWF under grid fault conditions becomes a vital problem [6]. After a grid fault occurs, the active power output capacity of the receiving end converter (REC) decreases substantially, and the surplus power accumulates on the DC transmission line. The DC bus voltage increases rapidly [7], which triggers overvoltage protection and causes the system to stop operating.

In most practical projects, energy dissipation equipment is used to deal with surplus wind power under grid-fault conditions. There are two different types of energy-dissipation equipment. The AC-type energy dissipation equipment generally adopts thyristors, which are installed on the AC side

The associate editor coordinating the review of this manuscript and approving it for publication was Elisabetta Tedeschi.

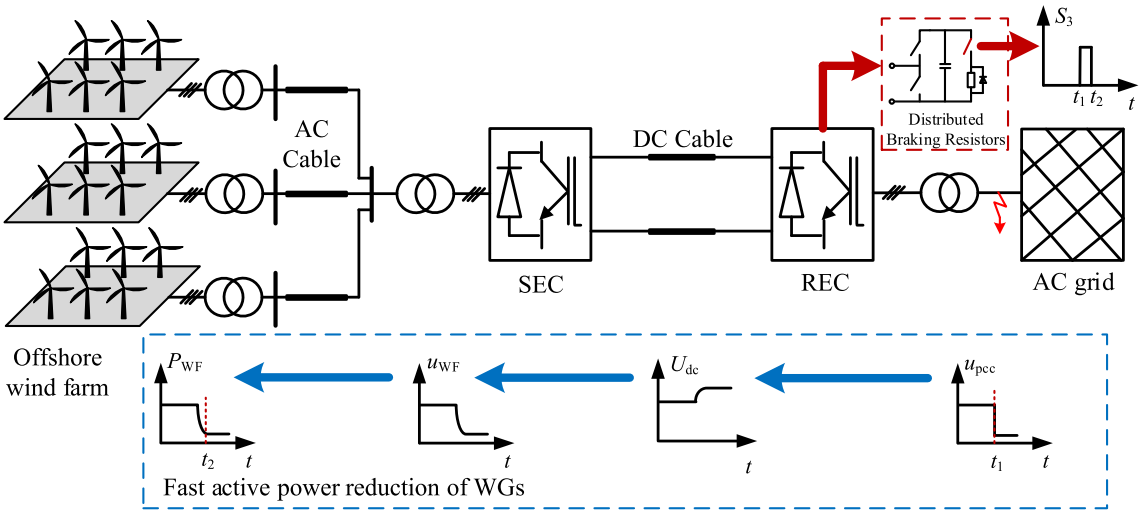

FIGURE 1. Overall LVRT strategy of MMC-HVDC system with wind farm integration.

of the sending end converter (SEC) and occupy a large area of the offshore platform. Therefore, they are not suitable for offshore wind farms. The DC-type energy dissipation equipment generally adopts IGBTs, which are installed at the DC side of the REC. The early energy dissipation equipment is composed of a series-connected IGBT valve and a braking resistor [8], [9]. The resistor is inserted and bypassed according to the DC voltage. However, with the increase in the voltage level, the voltage balancing of a large number of series-connected IGBTs has become a technical bottleneck. Recently, the dynamic braking system (DBS) [10], [11], [12], [13], [14] has been widely utilized in HVDC projects, in which the series-connected IGBT valve is replaced by series-connected submodules. The DBSs have three different types according to the arrangement of braking resistors: centralized DBS (applied in the Rudong Project), distributed DBS (applied in the Borwin2 project), and hybrid DBS.

Considering the worst case, that is, the output active power of the REC drops to 0 and the wind power is rated, the capacity of the energy dissipation equipment should be equal to the rated wind power, which is very large. Therefore, an independent station is required for DBS. Capacitors in the DBS also increase the volume and cost of the station. As a result, the construction cost of the energy dissipation station is approximately 1/7–1/6 that of the main REC station.

To reduce the cost of energy dissipation equipment, some scholars have proposed that the output power of a wind farm can be rapidly reduced to match the output power limit of the REC when the power grid fails. The communication-based coordination method is adopted from literature [15], [16]. When low-voltage faults occur in the power grid, the wind farm can rapidly reduce its output power by sending instructions via communication. Considering the cost, reliability, delay, and other problems of communication methods, the fault ride-through strategy without communication has been adopted in the literature [17], [18], [19], [20]. In these methods, when the DC-link voltage exceeds the threshold, the SEC reduces the AC voltage or increases the frequency of the wind farm. Then the wind turbines are controlled to reduce the active power output. However, owing to the small inertia of the DC system, DC-side overvoltage may trigger protection within tens of milliseconds. Therefore, the time requirement for wind farm power reduction is very strict, which makes it difficult to guarantee the reliability of such methods.

To balance the cost and reliability, a novel LVRT strategy is proposed in this paper. The "buffer" braking resistors are distributed in the submodules of the REC. These resistors are only required to dissipate surplus power at the early stage of the LVRT process (<200ms). Simultaneously, the wind farm voltage is rapidly reduced by the SEC, triggering the LVRT protection of the wind turbine. The output active power of the wind farm can be reduced, and the braking resistors in the REC submodules are gradually bypassed. This method does not need to build additional energy dissipation stations and greatly reduces the cost. Finally, an MMC-HVDC transmission system with OWF integration is constructed in the RT-Lab platform. The effectiveness of the proposed LVRT strategy is verified.

II. THE OVERALL COORDINATED LVRT STRATEGY OF THE MMC-HVDC SYSTEM AND WIND FARM

The overall coordinated LVRT strategy is illustrated in Fig. 1. When a fault occurs at $t = t_1$, the rapid increase in the DC voltage activates two different control loops:

1) The energy dissipation equipment is activated and utilized to dissipate the surplus power;
2) The SEC rapidly reduces the AC voltage, which triggers the LVRT of the WGs. The output active power of the WGs is reduced at $t = t_2$.

It can be observed that the energy-dissipation equipment operates only between t_1 and t_2. With this coordination

strategy, the surplus wind power absorbed by the energy-dissipation equipment is significantly reduced. Therefore, the braking resistors of the energy-dissipation equipment can be integrated and distributed into the submodules of the REC station, as shown in Fig.2. A ''buffer'' circuit is parallel connected to the submodule capacitor of the REC. The ''buffer'' circuit consists of an IGBT, a braking resistor, and a free-wheeling diode. When the IGBT S_3 is switched on, the submodule capacitor discharges and the braking resistor dissipates the surplus power. The total dissipated power can be flexibly controlled by varying the total number of inserted braking resistors.

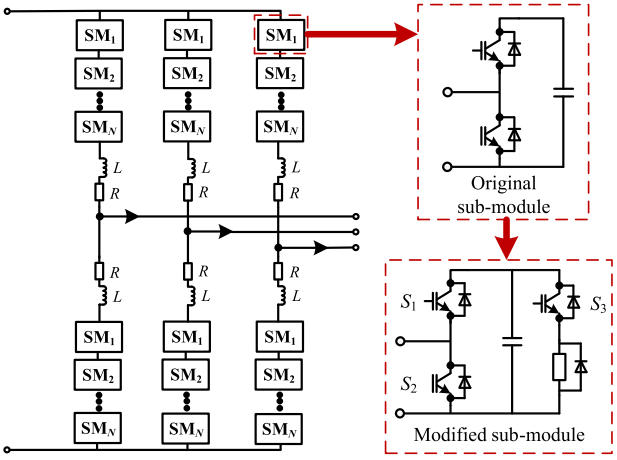

FIGURE 2. Topology of MMC-based REC station with original submodules and modified submodules with distributed braking resistors.

With the proposed LVRT strategy, the large energy dissipation station is replaced by distributed braking resistors in the submodules of the REC, which can significantly reduce the construction cost of the MMC-HVDC system with OWF integration.

The rest of this paper is organized as follows: The design and control of the distributed braking resistors are introduced in *Section III*. The active power reduction control of the MMC-HVDC system and the wind farm is introduced in *Section IV*. The feasibility of integrating the braking resistors into the REC submodules is studied in *Section V*. *Section VI* compares the proposed method with different kinds of existing energy dissipation equipment. Simulation verification based on the RT-Lab platform is shown in *Section VII*. *Section VIII* draws some conclusions.

III. THE DESIGN AND CONTROL OF DISTRIBUTED BRAKING RESISTORS

Given that the number of submodules per bridge arm of the REC station is N, where the number of redundant submodules is N_R, the maximum DC voltage is u_{dcmax} (usually 1.1 times the rated DC voltage), and the rated power is P_{nom}, it is known that the maximum voltage of each submodule capacitor is $u_{dcmax}/(N\text{-}N_R)$. There are 6 $(N\text{-}N_R)$ power buffer submodules to handle the surplus wind power, and the remaining 6 N_R submodules are used for redundancy. Considering the worst case, that is, the surplus wind power equals the rated power of the MMC-HVDC system, the surplus power to be handled by each submodule is $P_{nom}/6(N\text{-}N_R)$, and the value of the distributed buffer resistor is

$$R = \frac{\left(u_{dcmax}/N - N_R\right)^2}{P_{nom}/6\,(N - N_R)} \tag{1}$$

In normal operation, the REC controls the DC voltage. However, during grid fault conditions, the active power output capability of the REC is largely decreased. If the wind power is greater than the active power output capability of the REC station, the DC voltage will rise rapidly. When the DC voltage exceeds 1.05p.u., the buffer resistor in the submodule is put into use and takes over the control of the DC voltage instead of the REC, as shown in Fig. 3.

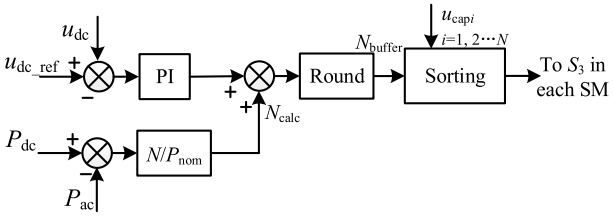

FIGURE 3. Control strategy of the distributed braking resistors.

The DC voltage u_{dc} can be controlled by adjusting the number of buffer resistors N_{buffer} inputs using a proportional-integral (PI) controller. The feedforward N_{calc} is introduced to speed up the insertion of distributed braking resistors at the initial stage of fault occurrence to avoid DC voltages exceeding the protection threshold. N_{calc} can also help cut off distributed braking resistors after the power reduction of the wind farm.

By integrating the braking resistors into the REC submodules, the MMC-HVDC system does not require an individual energy dissipation station, which takes up a large area. However, the operating time of the braking resistors should not be too long, or the dissipated power will significantly influence the thermal design of the REC submodules. Therefore, coordinated control of the MMC-HVDC system and the OWF is proposed to rapidly reduce the output active power of the WGs.

IV. THE FAST ACTIVE POWER REDUCTION CONTROL OF THE MMC-HVDC SYSTEM AND WIND FARM

For full-scale converter-based WGs, a DC chopper is widely used to solve the LVRT problem when the WGs are connected to the grid via AC transmission. The chopper is utilized to absorb excess power and is activated when the DC-link voltage surpasses the predefined threshold. However, when the WGs are integrated into the onshore AC grid via the MMC-HVDC transmission system, they cannot sense the grid fault, and the DC choppers in the WGs do not work.

Therefore, the LVRT capability of the choppers is not fully utilized.

As shown in Fig. 1, to make full use of the de-loading capabilities of the WGs, the SEC is controlled to reduce its AC voltage when the HVDC voltage exceeds the threshold. This triggers the LVRT control of the WGs, and the DC choppers in the WGs are inserted to consume the surplus power. The details of the coordinated active power reduction control are introduced in this section.

A. ACTIVE POWER LIMIT OF THE REC UNDER GRID FAULT

The control of the REC is shown in Fig.4. u_{dc} and u_{dcref} are the measured and reference values of the DC voltage, respectively. Q and Q_{ref} are the calculated and reference value of the output reactive power, respectively. u_{PCC} is the AC voltage at the point of common coupling. i_{REC} is the output current of the REC. i_{abcp} and i_{abcn} are the three-phase arm current at the upper arm and lower arm, respectively. The conventional double-closed-loop control is utilized to control the DC voltage and the output reactive power. The nearest level modulation (NLM) is applied to generate the gate signal for the submodules of the REC [24]. The sorting method based on the direction of arm current is utilized to ensure the balancing of the submodule capacitors. The circulating current suppressing controller (CCSC) utilizes a PI controller in a double-frequency rotating reference frame to suppress the second-order circulating current [25].

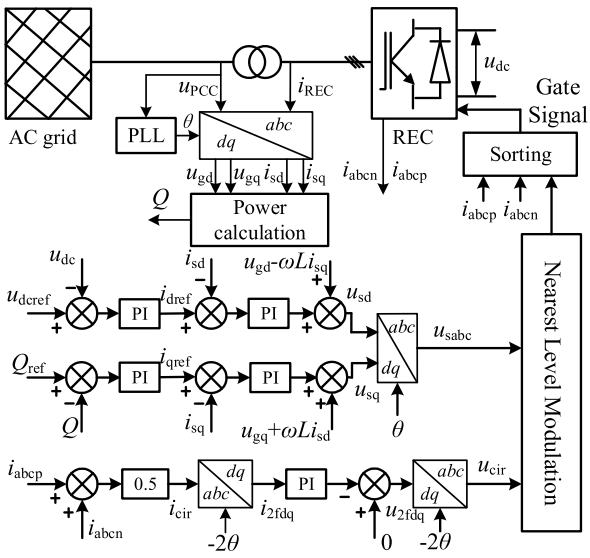

FIGURE 4. Control diagram of the REC.

When a grid fault occurs, the REC is required to provide reactive current support to the grid, according to the standard such as [21]:

$$i_{qref}=1.5i_{nom}(0.9-\frac{u_g}{u_{gnom}})0.2u_{gnom}\le u_g<0.9u_{gnom} \quad (2)$$

where i_{nom} is the rated current of the REC.

Therefore, the upper limit of active current i_{dmax} is:

$$i_{d\,max}=\sqrt{i_{lim}^2-i_{qref}^2} \quad (3)$$

where i_{lim} is the maximum output current of the REC, which is usually 1.2p.u.. The active power limit of the REC is

$$P_{max}=u_g i_{d\,max} \quad (4)$$

Considering the worst condition in the standard, that is, the grid voltage drops to 0.2p.u., the minimum output active power of the REC is approximately 0.12p.u..

During the fault, the active power output capability of the REC is largely reduced, especially when the reactive current support is applied. The surplus power leads to the increase of the DC voltage. Then the distributed braking resistors will be put in. At the same time, the AC voltage reduction control of the SEC will be activated.

B. AC VOLTAGE REDUCTION OF THE SEC

The SEC usually operates in the V/f control mode, that is, by controlling the AC voltage and frequency of the wind farm. Commonly used strategies include open-loop, AC voltage single closed-loop, and AC voltage-AC current double closed-loop. Although the open-loop and AC voltage single closed-loop control can reduce the AC voltage more quickly, the absence of a current loop can easily lead to SEC overcurrent. Double closed-loop control can protect the REC from overcurrent. However, a physical capacitance is required at the AC side of the SEC to decouple the outer AC voltage loop and the inner AC current loop in the double closed-loop control. For the MMC, there is no filter capacitance on the AC side. Thus, the performance of the double-closed-loop control may degrade [22], [23].

To solve this problem, AC current-loop control with virtual impedance is utilized, as shown in Fig.5. The AC voltage error is divided by the virtual impedance to obtain the AC current reference value. A circular current limiter is used to restrict the AC current reference to avoid exceeding the current limitation. Then a current loop is utilized to generate the output AC voltage reference u_{WFabc} of the SEC. The modulation method, submodule capacitor balancing method, and CCSC of the SEC are the same as the REC.

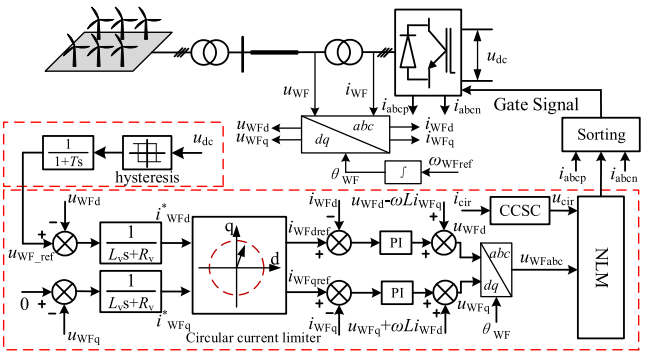

FIGURE 5. AC voltage reduction control of the SEC.

$u_{\mathrm{WF\_ref}}$ and u_{WF} are the reference and measured values of the wind farm voltage. i_{WF} is the measured value of the current of the SEC. L_{v} and R_{v} are the value of the virtual reactance and virtual resistance, respectively. ω_{WFref} is the reference frequency of the wind farm. The detailed structure of the circular current limiter is shown in Eq. (5). i_{lim} is usually set to 1.2∼1.5 p.u., according to the overcurrent capability of the SEC.

$$\begin{cases} i_{\mathrm{WFdref}} = i^*_{\mathrm{WFd}} \\ i_{\mathrm{WFqref}} = i^*_{\mathrm{WFq}} \end{cases} \quad \text{if } \sqrt{i^{*2}_{\mathrm{WFd}} + i^{*2}_{\mathrm{WFq}}} \le i_{\mathrm{lim}}$$
$$\begin{cases} i_{\mathrm{WFdref}} = \dfrac{i^*_{\mathrm{WFd}} i_{\mathrm{lim}}}{\sqrt{i^{*2}_{\mathrm{WFd}} + i^{*2}_{\mathrm{WFq}}}} \\ i_{\mathrm{WFqref}} = \dfrac{i^*_{\mathrm{WFq}} i_{\mathrm{lim}}}{\sqrt{i^{*2}_{\mathrm{WFd}} + i^{*2}_{\mathrm{WFq}}}} \end{cases} \quad \text{if } \sqrt{i^{*2}_{\mathrm{WFd}} + i^{*2}_{\mathrm{WFq}}} > i_{\mathrm{lim}} \tag{5}$$

When the DC voltage exceeds the limit, e.g., 1.05p.u., the SEC changes the reference of the AC voltage to 0.2p.u.. To further avoid overcurrent to both the SEC and WGs, the rate of AC voltage reduction is limited by the 1st order filter. The time constant T_1 is set to 50ms, which is slower than that of the control loop of the SEC and wind power converters. In addition, a hysteresis unit is also used to avoid oscillations and misoperation. Considering the stability and the overcurrent capability of the SEC, the AC voltage reduction process is set to last for 150ms.

C. ACTIVE POWER REDUCTION OF THE WG

Taking the permanent magnet synchronous generator-based WG as an example, the grid-side converter controls the DC bus voltage of the converter $U_{\mathrm{dc\_WT}}$, and the machine-side converter follows maximum power point tracking (MPPT) control. When the AC voltage $\underline{u}_{\mathrm{WF}}$ of the wind farm drops below 0.9 p.u., the active power reduction of the WG starts. According to the calculations in *Section IV.A*, the minimum active power output of the REC is 0.12p.u.. To match this limit, the maximum output power of the WG is set to 0.12p.u.. At this time, the grid-side converter of the WG almost does not output active power, and surplus wind power is accumulated on the DC-link capacitor of the wind power converter, which increases the DC-link voltage. At this time, the DC choppers in the WGs are activated to dissipate surplus wind power, and the distributed braking resistors in the REC can be bypassed. From the occurrence of grid faults to the completion of the WGs' power reduction, it takes less than 200ms, i.e., the distributed braking resistors need to work less than 200ms.

D. COORDINATION SEQUENCE OF THE MMC-HVDC SYSTEM AND THE OWF

This subsection introduces the coordination sequence among the REC, the SEC, and WGs. When detecting the dip of the PCC voltage, the REC provides reactive current to the grid according to the standard. If the wind power is greater than the residual power limit of the REC at this time, the DC voltage will continue to rise until it is higher than 1.05p.u. and the distributed braking resistors in the REC are inserted. At this point, the "buffer" loop takes over the control of the DC voltage and sets the reference value of the DC voltage to 1.06p.u..

Then, when the DC voltage detected by the SEC exceeds 1.05p.u., the AC voltage of the SEC will be gradually reduced to 0.2p.u., triggering the LVRT of the WGs and reducing the output active power of the wind farm. When the REC detects the DC-side power decline, the braking resistors are gradually bypassed and return the control of the DC voltage to the main control loop of the REC. Before the PCC voltage recovers, the REC needs to control the DC voltage at 1.06p.u to ensure that the SEC controls the AC voltage at 0.2p.u..

If the grid fault is recovered within a specified time, the REC adjusts the DC voltage to 1p.u., and the SEC gradually increased its AC voltage to 1p.u.. The MMC-HVDC system and wind farm can resume their normal operation. If the grid fault is not recovered within the specified time, the REC and SEC open the AC-side breaker, and the pulse will be blocked. The entire system stops its operation.

V. FEASIBILITY ANALYSIS OF INTEGRATING BRAKING RESISTOR INTO THE REC

According to the coordinated control strategy of the wind farm, the distributed braking resistor can be cut off when the DC chopper of the wind turbine is in operation. Thus, the distributed braking resistor only needs to operate for a short period to deal with the surplus power at the beginning of the grid fault. Therefore, the calorific value of the distributed braking resistor is very small.

Taking the parameters in the appendix as an example, when the HVDC transmission system works in the full-power mode, the surplus power in every MMC module can be calculated as follows:

$$P = {}^{P_{\mathrm{nom}}}\!/_{6\,(N - N_{\mathrm{R}})} = 437.4\mathrm{kW} \tag{6}$$

According to the analyses in *Section II*, the distributed braking resistor needs to work for 200ms before the DC chopper of the wind turbine is operated. The calorific value is calculated as follows:

$$Q = Pt \approx 87.5\mathrm{kJ} \tag{7}$$

According to the existing HVDC project, the allowable time interval of the braking resistor is 20 min. Therefore, the heat can be released in 20 min, and the average dissipation power can be calculated as

$$P_{\mathrm{dis}} = \frac{87.5\mathrm{kJ}}{1200\mathrm{s}} = 0.073\mathrm{kw} \tag{8}$$

The loss rate of receiving-end MMC is approximately 1.5%. Thus, the average dissipation power of every MMC submodule can be calculated as

$$P_{\mathrm{SM}} = \frac{0.015 P_{\mathrm{nom}}}{6\,(N - N_R)} = 6.56\mathrm{kW} \tag{9}$$

Comparing equations (8) and (9), the thermal power of the braking resistor is approximately 1/90 of that of the original MMC submodule. Therefore, it can be concluded that the distributed braking resistor has little influence on the thermal management of the MMC submodule, and the feasibility of the distributed braking resistor is confirmed.

To further avoid the influence on the thermal management of the MMC module, the braking resistor is wrapped into a material with high heat capacity, that is, ceramic or mica, and the heat is released slowly. If ceramic is selected as the heat-barrier material, the specific heat capacity is 850J/(kg·K). To limit the temperature to 500 °C to protect the resistor, the weight of the ceramic needs to be higher than 0.2 kg, which is not very large for a submodule.

VI. COMPARATIVE ANALYSIS WITH THE EXISTING DYNAMIC BRAKING SYSTEM

Three types of dynamic braking systems (DBSs) for MMCs are illustrated in Fig. 6. As the series-connected IGBT valve faces significant challenges in high-voltage application conditions, it is not analyzed in this section. All three topologies in Fig. 6 increase the voltage level and capacity of the DBS using a modular multilevel topology. In addition, du/dt and di/dt are restrained.

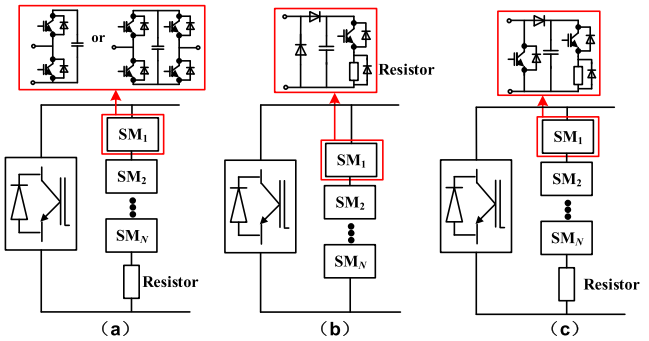

FIGURE 6. Typical topologies of energy dissipation equipment: (a) Centralized DBS (b) Distributed DBS (c) Mixed-type DBS.

As shown in Fig. 6(a), the submodules and centralized braking resistor are connected in series in the centralized DBS. Both half-bridge (HB) and full-bridge (FB) submodules can be utilized. In Fig. 6(b), the braking resistors are distributed in every submodule in the distributed DBS. In mixed-type MMC-DBS in Fig. 6(c), both centralized and distributed braking resistors are utilized.

For a centralized DBS, the dissipation power is controlled by adjusting the voltage on the centralized braking resistor, which depends on the number of inserted submodules. Assuming that there are N submodules in each arm of the REC, more than $2N$ IGBTs and N capacitors are needed in centralized HB-DBS. In addition, $4N$ IGBTs and N capacitors are required in centralized FB-DBS.

For a distributed DBS, the dissipation power can be adjusted flexibly by changing the number of inserted resistors. The burden of the submodule's water-cooling system is heavy in this topology, which enlarges the equipment size and increases the cost. In a distributed DBS, N IGBTs and N capacitors are needed.

The characteristics of centralized DBS and distributed DBS are combined in mixed-type MMC-DBS. The centralized resistor undertakes the main dissipation power, and every submodule contains a small resistor to maintain the balance of the capacitor voltage. $2N$ IGBTs and N capacitors are needed for mixed-type DBS.

From the analyses above, it can be seen that many capacitors are needed in all three kinds of DBSs, which will enlarge the equipment and increase the cost. Additionally, independent valve towers must be built. Therefore, the construction cost of the existing MMC-DBS is very high.

The proposed fault ride-through strategy uses the DC chopper of the WGs to consume surplus power by decreasing the SEC voltage during grid faults. Therefore, the operation time of the braking resistor can be effectively decreased, and the braking resistor has little influence on the thermal management of the MMC submodule, which lays the foundation for the resistor to be integrated and distributed into the REC submodules. Compared with the conventional DBS, the proposed LVRT strategy does not require extra capacitors or valve towers. In addition, the MMC submodule voltage is more stable when the braking resistor is put into operation during a grid fault, which further ensures the reliability of the system. Although the number of IGBTs used in the proposed strategy is much larger, which is $6N$, the rated current of every IGBT is very small (i.e., only $P_{\mathrm{nom}}/6U_{\mathrm{dc}}$). P_{nom} and U_{dc} are the rated active power and DC voltage, respectively, of the REC.

Therefore, it can be concluded that the proposed LVRT strategy for the MMC-HVDC transmission system with OWF integration based on distributed braking resistors is cheaper and more reliable than the existing MMC-DBS.

TABLE 1. Comparison of different types of energy dissipation equipment.

Type	Number of IGBTs	Rated voltage of each IGBT	Rated current of each IGBT	Number of capacitors
Centralized HB-DBS	$>2N$	U_{dc}/N	$P_{\mathrm{nom}}/U_{\mathrm{dc}}$	$>N$
Centralized FB-DBS	$4N$	U_{dc}/N	$P_{\mathrm{nom}}/U_{\mathrm{dc}}$	N
Distributed DBS	N	U_{dc}/N	$P_{\mathrm{nom}}/U_{\mathrm{dc}}$	N
Mixed-type DBS	$2N$	U_{dc}/N	$P_{\mathrm{nom}}/U_{\mathrm{dc}}$	N
Proposed distributed braking resistors	$6N$	U_{dc}/N	$P_{\mathrm{nom}}/6U_{\mathrm{dc}}$	0

VII. SIMULATION VERIFICATION

A. INTRODUCTION TO THE SIMULATION MODEL

To verify the effectiveness of the proposed LVRT strategy, a real-time simulation model based on Fig. 1 is built in the

RT-Lab platform in Fig. 7. The simulation model consists of two MMC stations, and the wind farm is aggregated into a 1000 MW PMSG. The detailed parameters of the MMC and PMSG can be found in Tables 2-3.

TABLE 2. Parameters of the HVDC converters.

Parameters	Value
Number of SMs per arm	412
Number of redundant SMs	31
SM capacitor	11mF
Rated DC voltage	±320kV
Rated AC voltage	333.13kV
Rated active power	1000MW
Rated reactive power	0Mvar
Arm reactance	80mH
DC side current limiting reactance	30mH
Transformer ratio (REC)	500kV/333.13kV
Rated power of the transformer (REC)	1400MVA
Leakage reactance of the transformer (REC)	16%
Transformer ratio (SEC)	230kV/333.13kV
Rated capacity of the transformer (SEC)	1400MVA
Leakage reactance of the transformer (SEC)	14%

TABLE 3. Parameters of the aggregated PMSG.

Parameters	Value
Rated capacity of the PMSG	1000MW
Rotor speed of the PMSG	4.2~11.9rad/s
Rated AC voltage	0.69kV
Rated wind speed	11.4m/s
Equivalent inertia of wind turbine	5.54s
Inertia of the generator	0.84s
DC-link voltage	1.1kV
Transformer ratio	0.69kV/35kV
Rated capacity of the transformer	1100MVA
Leakage reactance of the transformer	10%
DC chopper resistor	0.00125Ω

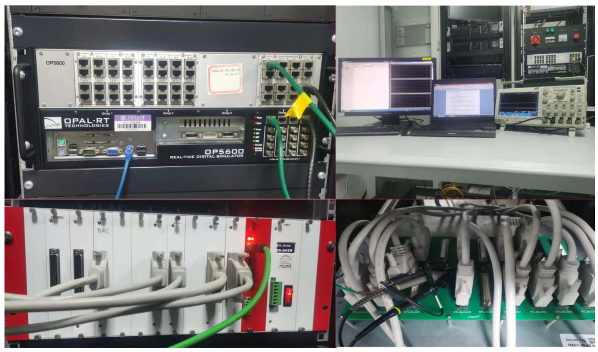

FIGURE 7. RT-LAB experiment platform.

The active power output of the wind farm is set to 800 MW. As shown in Fig.8, the grid voltage suddenly drops from 1 p.u. to 0.2p.u. at $t = 0.6$s, and recovers to 1 p.u. at $t = 1.2$s. Two different cases are simulated and compared.

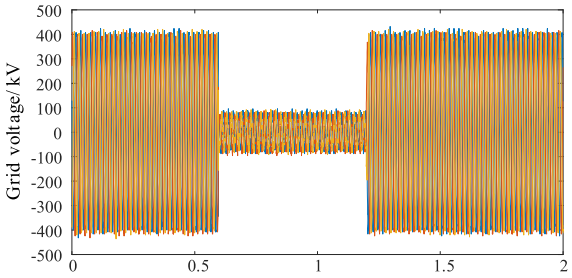

FIGURE 8. Grid voltage.

In Case A, only the fast active power reduction control is applied. In Case B, both fast active power reduction control and the distributed braking resistors (DBRs) are applied.

B. SIMULATION RESULTS

The responses of the REC and SEC in both cases are shown in Fig. 9 and Fig. 10. When the fault occurs at $t = 0.6$s, the active power output capability of the REC is largely reduced (see Fig. 9(c)). Without using DBRs, the DC voltage will rise quickly (see Fig. 9(a)). The DC-side overvoltage triggers the AC voltage reduction control of the SEC (see Fig.10(a)). Then the LVRT control of the wind turbine is activated. The output active power of the wind farm is reduced in approximately 200ms (see Fig.10(c)), and the DC voltage will stop increasing (see Fig. 9(a)). During this process, the AC side input current of the SEC does not exceed the limit. It can be found that the active power reduction control of the SEC and the wind farm is effective.

However, without using DBRs, the DC voltage increases to around 1000kV in 200ms, which largely exceeds the limit value of the overvoltage protection. Therefore, using only the active power reduction method cannot realize LVRT under severe grid faults.

When the DBRs are utilized, it can be found that the rising of DC voltage is constrained (see Fig. 9(a)). The DC voltage is controlled to 1.06p.u. This value does not trigger the overvoltage protection but triggers the AC voltage reduction control of the SEC (see Fig.10(a)). After 200ms, the output active power of the wind farm is reduced. The internal DC choppers of the wind turbines are activated to dissipate the surplus power, and the DBRs are gradually deactivated. With both DBRs and the active power reduction control, the DC voltage can remain stable during the LVRT process. When the grid fault recovers, the DC voltage recovers first. Then the AC voltage of the wind farm is controlled back to the rated value. And the output active power of the wind farm also recovers. The system can be restored to normal operation. The effectiveness of the proposed coordinated LVRT strategy is verified.

During the LVRT process, the number of the inserted DBRs is shown in Fig. 11. It can be found that the DBRs are only inserted in the beginning 200ms, which coincides with the analysis in *Section II*. The active power reduction control of the SEC and the wind farm can reduce the inserted time of

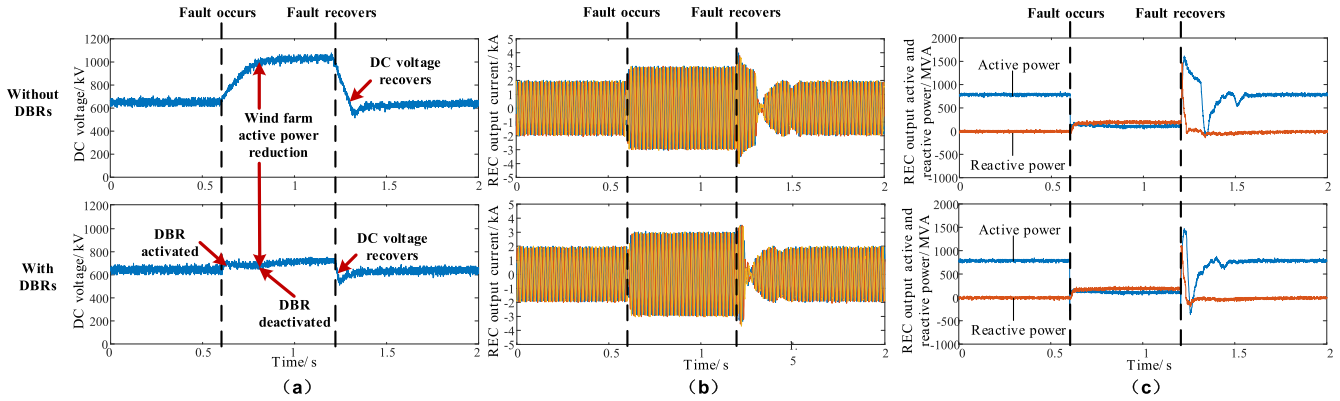

FIGURE 9. Waveforms of the REC: (a) DC voltage (b) REC output current (c) REC output active and reactive power. (Upper panel: without DBR; lower panel: with DBR.)

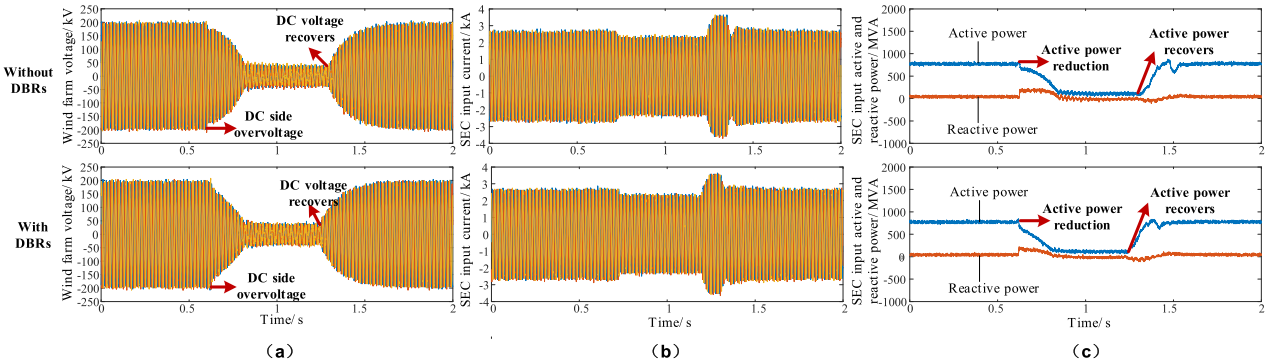

FIGURE 10. Waveforms of the SEC: (a) Wind farm voltage (b) SEC output current (c) SEC input active and reactive power. (Upper panel: without DBR; lower panel: with DBR.)

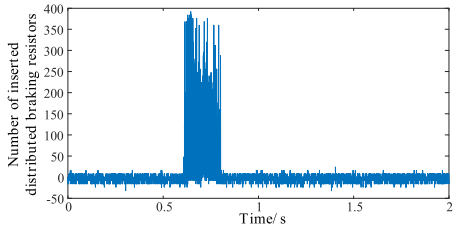

FIGURE 11. Number of inserted distributed braking resistors.

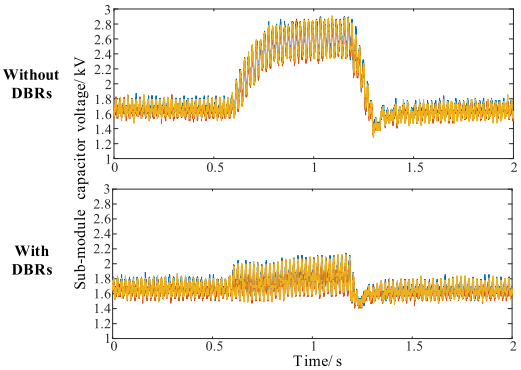

FIGURE 12. Submodule capacitor voltage waveforms.

the DBRs, thus making it possible to put the DBRs into the submodules of the REC.

In addition, the capacitor voltage waveforms of three different submodules in phase A of the REC are shown in Fig. 12. It can be found that the voltage ripples of the submodule capacitors are similar in both cases under normal and fault conditions. The insertion of DBRs does not increase the voltage ripple of the submodule capacitors.

VIII. CONCLUSION

Aiming at the OWF integrated into the grid via MMC-HVDC transmission, this paper proposes an LVRT strategy based on the coordination of "buffer" braking resistors distributed in REC's submodules and WGs' DC choppers, which have the following characteristics:

1) High reliability: The surplus power is consumed by the distributed "buffer" resistors at the early stage of the grid fault, so that the WG has a relatively generous time to reduce its output active power, avoiding DC overvoltage.
2) Low cost: the "buffer" resistors are distributed in the submodules of the REC, and they only work for a short period. Compared with the existing energy dissipation equipment, no extra capacitor is needed, and no individual energy dissipation station is required, which can significantly reduce the cost.

3) Protection of submodules: Buffer resistors are installed in each submodule of the REC, which can protect the capacitor of each submodule from overvoltage during not only the grid fault but also the normal operation of the REC.

Finally, simulation studies in RT-Lab show that the proposed strategy can control the DC voltage stably and realize a reliable LVRT of the OWF and MMC-HVDC system during the grid fault.

The RT-Lab simulation results have shown the effectiveness of the proposed method under symmetrical grid faults. The feasibility of the method under unbalanced grid faults will be further studied in the future.

REFERENCES

[1] J. Lee, "GWEC. Global wind report 2021," Global Wind Energy Council, Brussels, Belgium Tech. Rep., Mar. 2021. [Online]. Available: https://gwec.net/global-wind-report-2021/
[2] G. Li, C. Li, and D. V. Hertem, "HVDC technology overview," in *HVDC Grids: For Offshore Supergrid Future*. Hoboken, NJ, USA: Wiley, 2016, pp. 45–78. [Online]. Available: https://onlinelibrary.wiley.com/doi/pdf/10.1002/9781119115243.ch3
[3] A. Reidy and R. Watson, "Comparison of VSC based HVDC and HVAC interconnections to a large offshore wind farm," in *Proc. IEEE Power Eng. Soc. Gen. Meeting*, vol. 1, Jun. 2005, pp. 1–8.
[4] N. Flourentzou, V. G. Agelidis, and G. D. Demetriades, "VSC-based HVDC power transmission systems: An overview," *IEEE Trans. Power Electron.*, vol. 24, no. 3, pp. 592–602, Mar. 2009.
[5] S. Debnath, J. Qin, B. Bahrani, M. Saeedifard, and P. Barbosa, "Operation, control, and applications of the modular multilevel converter: A review," *IEEE Trans. Power Electron.*, vol. 30, no. 1, pp. 37–53, Jan. 2015.
[6] G. Li, J. Liang, F. Ma, C. E. Ugalde-Loo, and H. Liang, "Analysis of single-phase-to-ground faults at the valve-side of HB-MMCs in HVDC systems," *IEEE Trans. Ind. Electron.*, vol. 66, no. 3, pp. 2444–2453, Mar. 2019.
[7] G. Ramtharan, A. Arulampalam, J. B. Ekanayake, F. M. Hughes, and N. Jenkins, "Fault ride through of fully rated converter wind turbines with AC and DC transmission," *IET Renew. Power Gener.*, vol. 3, no. 4, pp. 426–438, Dec. 2009.
[8] C. Nentwig, J. Haubrock, R. H. Renner, and D. Van Hertem, "Application of DC choppers in HVDC grids," in *Proc. IEEE Int. Energy Conf. (ENERGYCON)*, Apr. 2016, pp. 1–5.
[9] S. K. Chaudhary, R. Teodorescu, P. Rodriguez, and P. C. Kjar, "Chopper controlled resistors in VSC-HVDC transmission for WPP with full-scale converters," in *Proc. IEEE PES/IAS Conf. Sustain. Alternative Energy (SAE)*, Valencia, Spain, Sep. 2009, pp. 1–8.
[10] J. Maneiro, S. Tennakoon, C. Barker, and F. Hassan, "Energy diverting converter topologies for HVDC transmission systems," in *Proc. 15th Eur. Conf. Power Electron. Appl. (EPE)*, Sep. 2013, pp. 1–10.
[11] C. C. Davidson and R. A. Mukhedkar, "A comparison of different types of dynamic braking system for HVDC systems for offshore wind power," in *Proc. CIGRÉ Brussels*, Brussels, Belgium, 2014, pp. 1–8.
[12] V. Hussennether, "Projects BorWin2 and HelWin1-large scale multi-level voltage-sourced converter technology for bundling of offshore wind power," in *Proc. CIGRÉ Session*, 2012, pp. 1–11, Paper B4-306.
[13] S. Cao, W. Xiang, X. Lu, W. Lin, K. Zhang, J. Wen, and X. Zhang, "Energy dissipation of MMC-HVDC based onshore wind power integration system with FB-DBS and DCCB," *IET Renew. Power Gener.*, vol. 14, no. 2, pp. 222–230, 2020.
[14] B. Xu, C. Gao, J. Zhang, J. Yang, B. Xia, and Z. He, "A novel DC chopper topology for VSC-based offshore wind farm connection," *IEEE Trans. Power Electron.*, vol. 36, no. 3, pp. 3017–3027, Mar. 2021.
[15] C. Feltes, H. Wrede, F. W. Koch, and I. Erlich, "Enhanced fault ride-through method for wind farms connected to the grid through VSC-based HVDC transmission," *IEEE Trans. Power Syst.*, vol. 24, no. 3, pp. 1537–1546, Aug. 2009.
[16] D. Tzelepis, A. O. Rousis, A. Dysko, and C. Booth, "Enhanced DC voltage control strategy for fault management of a VSC-HVDC connected offshore wind farm," in *Proc. 5th IET Int. Conf. Renew. Power Gener. (RPG)*, 2016, pp. 1–6.
[17] R. T. Pinto, P. Bauer, S. F. Rodrigues, E. J. Wiggelinkhuizen, J. Pierik, and B. Ferreira, "A novel distributed direct-voltage control strategy for grid integration of offshore wind energy systems through MTDC network," *IEEE Trans. Ind. Electron.*, vol. 60, no. 6, pp. 2429–2441, Jun. 2013.
[18] A. Kirakosyan, M. S. E. Moursi, and V. Khadkikar, "Fault ride through and grid support topology for the VSC-HVDC connected offshore wind farms," *IEEE Trans. Power Del.*, vol. 32, no. 3, pp. 1592–1604, Jun. 2017.
[19] C. Liu, F. Deng, Q. Heng, X. Cai, R. Zhu, and M. Liserre, "Crossing thyristor branches-based hybrid modular multilevel converters for DC line faults," *IEEE Trans. Ind. Electron.*, vol. 68, no. 10, pp. 9719–9730, Oct. 2021.
[20] Y. Jing, R. Li, L. Xu, and Y. Wang, "Enhanced AC voltage and frequency control of offshore MMC station for wind farm connection," *IET Renew. Power Gener.*, vol. 12, no. 15, pp. 1771–1777, Nov. 2018.
[21] *Technical Rule Connecting Wind Farm to Power System: GB/T 19963-2011*, China Electr. Council, Beijing, China, 2011.
[22] C. Zhang, X. Cai, A. Rygg, and M. Molinas, "Sequence domain SISO equivalent models of a grid-tied voltage source converter system for small-signal stability analysis," *IEEE Trans. Energy Convers.*, vol. 33, no. 2, pp. 741–749, Jun. 2018.
[23] M. G. Taul, X. Wang, P. Davari, and F. Blaabjerg, "Current limiting control with enhanced dynamics of grid-forming converters during fault conditions," *IEEE Trans. Emerg. Sel. Topics Power Electron.*, vol. 8, no. 2, pp. 1062–1073, Jun. 2020.
[24] K. Sharifabadi, L. Harnefors, H.-P. Nee, S. Norrga, and R. Teodorescu, *Design, Control and Application of Modular Multilevel Converters for HVDC Transmission Systems*, 1st ed. Hoboken, NJ, USA: Wiley, 2016.
[25] Q. Tu, Z. Xu, and L. Xu, "Reduced switching-frequency modulation and circulating current suppression for modular multilevel converters," *IEEE Trans. Power Del.*, vol. 26, no. 3, pp. 2009–2017, Jul. 2011.

XIAOHE WANG received the B.S. and Ph.D. degrees in electrical engineering from Zhejiang University, Hangzhou, China, in 2014 and 2019, respectively.

From 2019 to 2021, he worked as a Postdoctoral Researcher with Powerchina Huadong Engineering Corporation Ltd., Hangzhou, cocultured by the College of Electronic Information and Electrical Engineering, Shanghai Jiao Tong University, Shanghai, China. He is currently engaged in researching the wind power generation and transmission system with Powerchina Huadong Engineering Corporation Ltd. His current research interests include model and control strategy of modular multilevel converter and wind power generator.

RENXIN YANG (Member, IEEE) received the B.Eng. degree in electrical engineering and automation from the Huazhong University of Science and Technology, Wuhan, China, in 2014, and the Ph.D. degree in electrical engineering from Shanghai Jiao Tong University, Shanghai, China, in 2020.

His current research interests include topology, control, active frequency response, and fault ride-through of MMC-based HVDC system with wind farm integration.

ZHAOHUI SHI received the B.S. degree in electrical engineering from Northeast Electric Power University, Jilin, China, in 2005.

He is currently working as the Vice President with the Renewable Energy Engineering Institute, Powerchina Huadong Engineering Corporation Ltd., Hangzhou, China. His current research interests include renewable energy power generation and transmission system design.

XU CAI (Senior Member, IEEE) received the B.Eng. degree from Southeast University, Nanjing, China, in 1983, and the M.Sc. and Ph.D. degrees from the China University of Mining and Technology, Xuzhou, China, in 1988 and 2000, respectively. He was with the Department of Electrical Engineering, China University of Mining and Technology, as an Associate Professor, from 1989 to 2001. He was the Vice Director of the State Energy Smart Grid Research and Development Center, Shanghai, China, from 2010 to 2013. He has been with Shanghai Jiao Tong University, Shanghai, as a Professor, since 2002, where he has been the Director of the Wind Power Research Center, since 2008. His current research interests include power electronics and renewable energy exploitation and utilization, including wind power converters, wind turbine control systems, large power battery storage systems, clustering of wind farms and its control systems, and grid integration.

XIANQIANG SHI (Graduate Student Member, IEEE) received the B.Sc. and M.Sc. degrees in electrical engineering from the China University of Mining and Technology, Xuzhou, China, in 2015 and 2018, respectively. He is currently pursuing the Ph.D. degree with the Department of Electrical Engineering, Shanghai Jiao Tong University, Shanghai, China.

His research interests include modular multilevel converters and high-voltage direct current technology.

YUWEI CHEN received the Ph.D. degree in electrical engineering from Zhejiang University, Hangzhou, China, in 2021.

Since 2021, she has been working as a Postdoctoral Researcher with Powerchina Huadong Engineering Corporation Ltd., Hangzhou, cocultured by the College of Electrical Engineering, Zhejiang University, Hangzhou. She is currently engaged in researching the optimization of wind farms and power systems with Powerchina Huadong Engineering Corporation Ltd. Her current research interest includes model and optimization algorithms of non-linear systems.